

Accepted Manuscript

Integration of Thin Film Bulk Acoustic Resonators onto Flexible Liquid Crystal Polymer Substrates

R.V. Wright, G. Hakemi, P.B. Kirby

PII: S0167-9317(11)00063-3
DOI: [10.1016/j.mee.2011.01.038](https://doi.org/10.1016/j.mee.2011.01.038)
Reference: MEE 7700

To appear in: *Microelectronic Engineering*

Received Date: 28 October 2010
Accepted Date: 14 January 2011



Please cite this article as: R.V. Wright, G. Hakemi, P.B. Kirby, Integration of Thin Film Bulk Acoustic Resonators onto Flexible Liquid Crystal Polymer Substrates, *Microelectronic Engineering* (2011), doi: [10.1016/j.mee.2011.01.038](https://doi.org/10.1016/j.mee.2011.01.038)

This is a PDF file of an unedited manuscript that has been accepted for publication. As a service to our customers we are providing this early version of the manuscript. The manuscript will undergo copyediting, typesetting, and review of the resulting proof before it is published in its final form. Please note that during the production process errors may be discovered which could affect the content, and all legal disclaimers that apply to the journal pertain.

Integration of Thin Film Bulk Acoustic Resonators onto Flexible Liquid Crystal Polymer Substrates

R.V. Wright, G. Hakemi, P.B. Kirby

Microsystems and Nanotechnology Centre, Cranfield University, Cranfield, Bedfordshire, UK

Abstract: Thin film bulk acoustic resonators (FBARs) have been directly integrated on liquid crystal polymer (LCP) substrates for application to the field of flexible electronics. Particular developments required were chemo-mechanical polishing for LCP roughness reduction to enable growth of high quality ZnO films and a through substrate deep reactive ion etch process. Q values of up to 126 and 78 for series and parallel resonances combined with an electromechanical coefficient (k_t^2) ~6.7% were achieved. Further device development is needed but this performance is already sufficient for some chemical/ biological sensing applications.

There is currently wide interest in the developing field of plastic electronics, both for applications where an extremely low unit cost is required for example RFid and also - through the ease of creating foldable structures - where space is at a premium e.g mobile phones, digital cameras¹. The use of polymer substrates is a key feature of this new technology and the extent to which conventional electronic devices can be integrated on them is being actively researched with a number of successes already demonstrated^{2,3}. The incorporation of microelectromechanical systems (MEMS) devices presents a still further challenge and it is the subject of the present work to directly integrate RF MEMS components, specifically thin film bulk acoustic resonators (FBARs), onto liquid crystal polymer (LCP) - an attractive substrate material for RF applications due to its excellent dielectric properties, low water absorption and dimensional stability^{4,5}. FBARs, which are normally fabricated on Si, are much used in duplexer filters for mobile phones, and with the increasing pressure on space and the consequent move towards the use of conformal antennas⁶ integration of the duplexer would, for example, be a crucial step towards complete integration of the RF front end in the antenna.

The conventional FBAR device is composed of a piezoelectric thin film, generally AlN or ZnO sandwiched between metal electrodes, e.g Au or Mo, and mechanically isolated from the Si substrate by etching away the Si from under the active area of the device as the final step of the process. The piezoelectric layer is almost universally RF magnetron sputtered and it is found that a low bottom electrode surface roughness is crucial to obtaining the highly preferred c-axis wurtzite crystal structure needed for device operation⁷. Since, as supplied, LCP has significant roughness, designed to enable good adhesion of deposited metal layers⁸, some form of surface smoothing was required and chemo-mechanical polishing (CMP) - already successfully demonstrated for other polymers^{9,10} - was chosen for this. For through substrate etching it was considered unlikely that device membranes could withstand the conventionally used laser ablation¹¹, and so a plasma etch process was developed, extending the techniques used up to now only for surface treatment¹². Lastly, although it is expected that roll-to-roll technology will be used for industrial-scale processing, for these initial investigations it was necessary to develop wafer bonding techniques to enable wafers to be kept flat during processing.

FBAR operation relies on RF signal excitation of thickness extensional mode acoustic vibrations in which the two faces of the piezoelectric film move in anti-phase. Device design and performance analysis are facilitated by use of the one dimensional solution of the governing coupled acoustic-electromagnetic equations for the electrical impedance¹³:

$$Z = \frac{1}{j\omega C_0} \left(1 - k_t^2 \frac{\tan(\phi)}{\phi} Y \right) \quad (1)$$

$$Y = \frac{z_1(jz_2 \tan(\phi_2) + jz_3 \tan(\phi_3) \cos^2(\phi_1) + jz_1^2 \sin(2\phi_1))}{z_1(z_2 + z_3) \cos(2\phi_1) + j(z_1^2 - z_2 \tan(\phi_2)z_3 \tan(\phi_3)) \sin(2\phi_1)} \quad (2)$$

$$k_t^2 = \frac{k_{33}^2}{(1 + k_{33}^2)} \quad \phi_i = \frac{\beta_i d_i}{2} \quad \beta_i = \frac{\omega}{V_i}$$

Where ω , C_0 , K_{33}^2 , are the angular frequency, geometric capacitance and electromechanical coupling coefficient and, with $i=1,2,3$ denoting piezoelectric and top and bottom electrode layers, V_i , Z_i , d_i , are the acoustic velocities, acoustic impedances and thicknesses of the layers, respectively. In the present work complex stiffness coefficients were assumed to take account of acoustic losses in the layers, leading to complex values for K_{33}^2 and the V_i (and hence ϕ_i , β_i) and Z_i . Dielectric loss in the ZnO was accounted for by using a complex permittivity in the defining equations for C_0 and K_{33}^2 . As is widely observed in bulk materials a quadratic frequency dependence was assumed for the acoustic losses. The above model was implemented in a MATLAB¹⁴ program in which literature values were taken for all the materials parameters for the initial design and the complex permittivity, ZnO acoustic loss and K_{33}^2 were used as the main fitting parameters for modeling of the fabricated devices.

FBARs having a Au/ZnO/Au layer structure were designed with fixed 100nm thick Au layers (thin, 10nm, Ti layers used to improve Au adhesion in fabricated devices were neglected in the modelling) and ZnO thickness (~1.0 μ m) selected to give resonant frequencies in the range 1.8-2.0 GHz. The devices were series configured in a conventional coplanar geometry with active areas ranging from 50x50 μ m² to 1x1mm² in 50 μ m steps to facilitate impedance matching of devices over a wide range of resonant frequencies (100 MHz to 3GHz) and a subset of these - the 50x50 to 150x150 μ m² devices - were used in the present work.

FBARs were fabricated on Ultralam 3850, a Cu clad LCP foil from Rogers Corporation¹⁵, using the processing route shown schematically in fig 1 (reference to which should be made in the following process description). To facilitate planar processing 4" diameter LCP disks were cut from the as received sheet and these were then bonded to Si backing wafers using Apiezon W wax¹⁶ as the adhesive. The key requirements for obtaining a flat surface after bonding - a uniform adhesive thickness and the application of a uniform pressure between the flexible LCP and a rigid flat plate during bonding - were achieved by spin-coating the wax (from a wax/toluene solution) onto both Si and LCP wafers to give a uniform thickness,

~10 μ m, and using a specially designed vacuum jig which enabled the wafers to be pressed uniformly against an optically flat plate by atmospheric pressure. For this latter step the assembly was placed on a hotplate at ~110°C, just above the wax softening point. Apiezon W wax was chosen both for its capability to withstand the temperatures and chemicals commonly used in micro-fabrication and also its vacuum compatibility. Following bonding, the top Cu layer was removed using a FeCl₃ solution. Chemo-mechanical polishing (CMP) was carried out using a Logitech CDP51 machine with pad type FastPad PPG (IC-1000 analogue) and a colloidal alumina slurry (Eminess Ultra-sol A12) dispensed at 20 ml/minute. With both platen and carrier speeds set to 50 rpm and a down force of 5 psi it was found that 20 minutes was required to completely polish the

LCP and achieve an acceptable polish with a roughness (Ra) value of ~5 nm. After polishing, the wafers were rinsed in distilled water and then placed in an ultrasonic bath filled with DI water. The Ti/Au./ZnO/Ti/Au layers composing the FBAR structure were deposited on the smoothed LCP sequentially using RF magnetron sputtering. The bottom electrode was patterned by wet etching using KI/I₂ and NHF₃/HNO₃ solutions for the Au and Ti layers, respectively, prior to ZnO deposition; vias through the ZnO to access the bottom electrode were wet etched in a 20% acetic acid solution; and the top electrode was patterned using a lift-off technique. Through substrate etching was then carried out by first etching vias through the Si by deep reactive ion etching (DRIE) in a STS Mesc Multiplex ICP plasma etcher and then removing the Apiezon wax and Cu at the bottoms of the vias by wet etching in toluene and a FeCl₃ solution, respectively. Finally the LCP was removed by further DRIE but using O₂ as process gas in place of the SF₆/C₄F₈, (Bosch) process gases used for the Si etching. The process was completed by solvent removal of the front- and back-side backing wafers with the latter retained initially to keep the wafer flat during RF measurements.

A completed device is shown in figure 2, the main features of which are a faint pock marking of the top electrode and deformation of the device membrane due to a high compressive thin film stress. The latter is also observed with Si based FBARs but is more extreme in this case leading to cracking of the membranes on most of the larger area (>150x150μm²) devices. The pock marking is not observed prior to LCP DRIE and is thought to be due to a very thin polymer residue. SEM measurements (figure 3) have shown that the LCP vias are quite well defined although there is a difficult to remove residue, traces of which can be seen on the sidewalls in the figure, which may be linked to the fibrillar structure of LCP.

RF measurements were carried out using a Hewlett Packard vector network analyzer (VNA) type 8753D with connection to the devices made using Cascade ACP40 GSG200 coplanar probes. Prior to device characterization the measurement set-up was calibrated to the probe tips using a short-open-line-through (SOLT) calibration procedure. Following S-parameter measurements, on- wafer test structures were used to de-embed the transmission line feeds to the devices. The de-embedded RF response of a 100x100μm resonator is shown in figure 4. The Q values at the measured series (f_s) and parallel (f_p) resonance frequencies (Q_s and Q_p) for this resonator, calculated from the 3dB bandwidths of the S₁₁ and S₂₁ minima, are Q_s=126 and Q_p=78 and the value of k_t² extracted from the modeling is 6.7%. Other extracted values are 8.4 for the dielectric constant (ε), 0.072 for the dielectric loss (tanδ) and 7613 N/m for the acoustic loss (at f_s). The k_t² and ε values are in the expected range for highly c-axis preferred orientation ZnO¹⁷. However, the Q_s and Q_p values are well below those routinely achieved with ZnO FBARs¹⁷ and it is believed that this is due mostly to an increase in acoustic scattering from a high density (~0.25/μm²) of outsized ZnO grains the presence of which has been revealed by atomic force microscopy (AFM) measurements (figure 5a). From previous experience these are most likely to have resulted from use of an insufficiently high ZnO growth temperature. In the present work this was limited to 100°C but with an alternative wafer bonding adhesive growth

in the 2-300°C range, as used for FBARs on Si, would be possible while still keeping the temperature below the melting point of the LCP (~315°C). Modelling suggests that the additional loss responsible Q_p being below Q_s is due to a high $\tan\delta$ which in turn could be due to a high ZnO conductivity. If so the conductivity would be given by $\omega\epsilon\tan\delta$, and substituting values from above, would amount to $6.7 \cdot 10^{-4} \Omega^{-1} \text{cm}^{-1}$ (at f_p), a value well above that of bulk ZnO but in the range for O_2 vacancy controlled conductivity¹⁸ suggesting that the O_2 partial pressure needs to be re-optimized for ZnO growth on LCP.

The potential for integration of functional ceramics onto flexible substrates has clearly been demonstrated and although further work is required to enable high Q applications such as duplexer filters for mobile phone to be addressed it is believed the performance of the present device would be adequate for some chemical and bio-medical sensing applications where operation is in a liquid environment and Q_s are performance not as high. Also, although the ZnO films have proved to be extremely resilient during handling following backing wafer removal it is expected that to achieve the flexibility already demonstrated for metal tracks on polymer, the ceramic, ZnO in this case, will need to be confined to the device area and connected to the substrate via strain relieving structures.

Acknowledgements

We thank Alan Blake of the Tyndall National Institute, University College Cork, Lee Maltings, Cork, Ireland for undertaking the CMP. This work was supported by the UK EPSRC (contract EP/D064783/1).

References

1. S.R.Forest, Nature (London) 428 (2004) 911-918.
2. L. Sun, G. Qin, H. Huang, H. Zhou, N. Behdad, W. Zhou and Z. Ma, Applied Physics Letters 96, (2010) 013509.
3. C. Liu, Adv. Mater. 19 (2007) 3783-3790.
4. D. Thompson, P. Kirby, J. Papapolymerou, M.M. Tentzeris, Proc. 53rd Electronic Components and Technology Conference (2003) 1652-1655.
5. X.F. Wang, J. Engel, C. Liu, J. Micromechanics and Microengineering 13 (5) (2003) 628-633.
6. J.C.G. Matthews, and G. Pettitt, Proceedings of the 3rd European Conf. on Antennas and Propagation, Berlin, Germany, Mar 23-27, 1-6 (2009) 246-250.
7. A. Artieda, M. Barbieri, C. S. Sandu, and P. Mural, Journal of Applied Physics 105(2) (2009) 024504.
8. M. Howlader, T. Suga, A. Takahashi, A. Saijo, S. Ozawa, and K. Nambu, International Conference on Intergranular and Interface Boundaries, Queens Univ., Belfast, Ireland, Mar 25-29, 2004, Journal of Material Science 40 (12) 3177-3184.

9. T. Ya-Li, D. Bau-Tong, T. Ming-Shih, T. I-Chung, and F. Ming-Shiann, International Symposium on VLSI Technology Systems and Applications, Taipei, Taiwan, 1999, Proceedings of Technical Papers. (Cat. No.99TH8453) 139-142.
10. Z.W. Zhong, Z.F. Wang, and B.M.P. Zirajutheen, Microelectronic Engineering 81(2005) 117 -124.
11. K.C. Yung, H. Liem, H. Choy, and T.M. Yue, Journal of Applied Polymer Science 116 (4) (2010) 2348-2358.
12. Y. Kurihara, H. Ohata, M. Kawaguchi, M. S. Yamazaki, and K. Kimura Journal of Applied Polymer Science 108 (1) (2008) 85-92.
13. C. Fragkiadakis, A. Luker, R.V. Wright, L. Floyd, and P.B. Kirby, 20th International Symposium on Integrated Ferroelectrics, Biopolis Singapore, Singapore, Jun. 2008, Journal of Applied Physics 105 (6) (2009) 061635.
14. Mathworks inc., Natick, MA, U.S.
15. Rogers Corporation, CT, U.S.
16. M&I Materials Ltd, Trafford Park, Manchester, U.K.
17. R. Aigner, Proceedings of the IEEE Custom Integrated Circuits Conference (2003) 141-146.
18. K.B.Sundaram and A. Khan, Thin Solid Films 295 (1-2), (1997) 87-91.

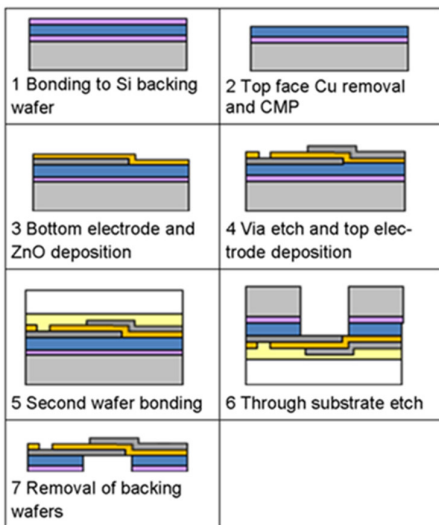
Figure 1 Process flow for fabrication of FBARs on LCP substrates

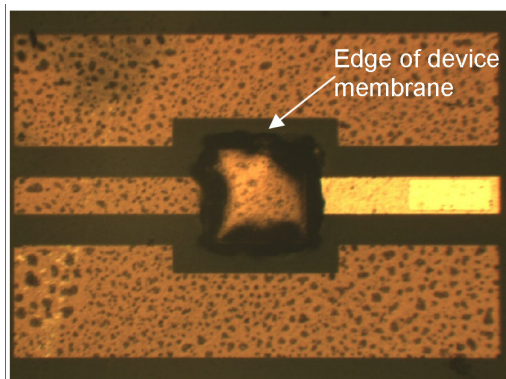
Figure 2 Optical micrograph of 150x150 μ m active area FBAR

Figure 3 SEM micrograph of LCP through substrate via.

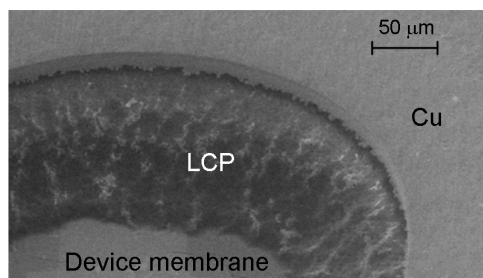
Figure 4 Modelled (dotted) and measured (solid line) RF response of a 100x100 μ m active area FBAR fabricated on LCP: a) magnitude, b) phase.

Figure 5 AFM image of ZnO grain morphology on a FBAR device fabricated on LCP

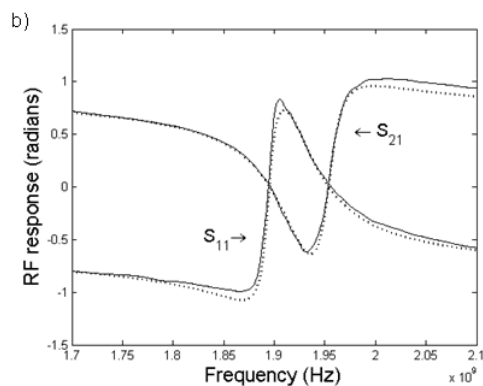
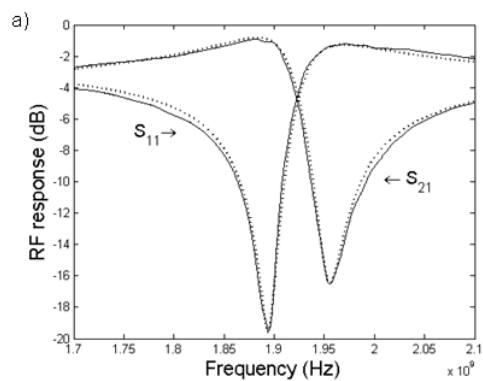


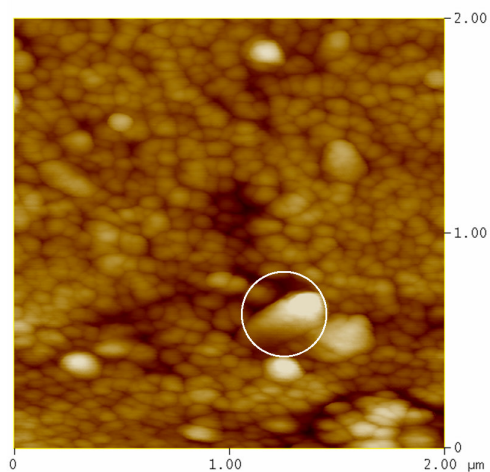


ACCEPTED MANUSCRIPT



ACCEPTED MANUSCRIPT





ACCEPTED MANUSCRIPT